Diffusion in Zeolites

DOI: 10.1002/anie.200705597

# Exploring Crystal Morphology of Nanoporous Hosts from Time-Dependent Guest Profiles**

*Despina Tzoulaki, Lars Heinke, Wolfgang Schmidt, Ursula Wilczok, and Jörg Kärger**

Nanoporous materials are key to a plethora of modern technologies and decisively contributed to the present boom in the development of heterogeneous catalysis and molecular sieves. In these applications, knowledge of the details of mass transport often turns out to be crucial for the exploration of routes for their use and further optimization. It was common practice to apply Fick's 1st law to analyze the rate of molecular uptake or release following a change in the pressure of the surrounding atmosphere.[1,2] This approach, however led to much smaller effective diffusion coefficients, which could only be attributed to the existence of transport resistance on the external surface of the crystal (that is, surface barriers, there are numerous models concerning their origin[3–7]). In addition there could be other barriers within the pore system of the zeolite bulk phase, acting in addition to the transport resistance.[8]

With the introduction of interference microscopy for monitoring time-dependent concentration profiles during molecular uptake and release,[9–14] the existence of these resistances could be confirmed by direct experimental evidence. These studies provided direct evidence of transport resistance on the external crystal surface (for crystal specimens of zeolite ZSM-5[11], ferierrite,[13] and the metal–organic framework (MOF) manganese formate[14]) and in the intracrystalline bulk phase (for zeolites of type CrAPO-5 and SAPO-5[12] and of ZSM-5/silicalite-1[9]). These findings were corroborated by the findings of two groups in recent investigations of the catalytic conversion on large ZSM-5 crystallites[15,16] which indicated the presence of intracrystalline diffusion barriers that notably influenced the overall reaction.

Herein, a specimen of a zeolite host system of type silicalite-1[17] could be identified where the influence of both surface barriers and internal barriers, such as interfaces and stacking faults, are found to be negligibly small in comparison with the transport resistance exerted by the regular intracrystalline pore system. In other words, in these silicalite-1 crystals, the transport properties that were found were those that were predicted from the established structure. Thus, predictions of the molecular transport, based exclusively on the regular pore structure, should reproduce the experimental diffusion coefficients.

Silicalite-1 crystals have a three-dimensional pore system, consisting of mutually intersecting straight (in crystallographic *b* direction) and zigzag (in crystallographic *a* direction) channels (Figure 1 a).[18–21] These are formed by a rapid growth along the crystallographic *c* axis during the early stages of the synthesis. As shown in Figure 1 b the crystallographic axes of segments 2 and 6 coincide with each other, and

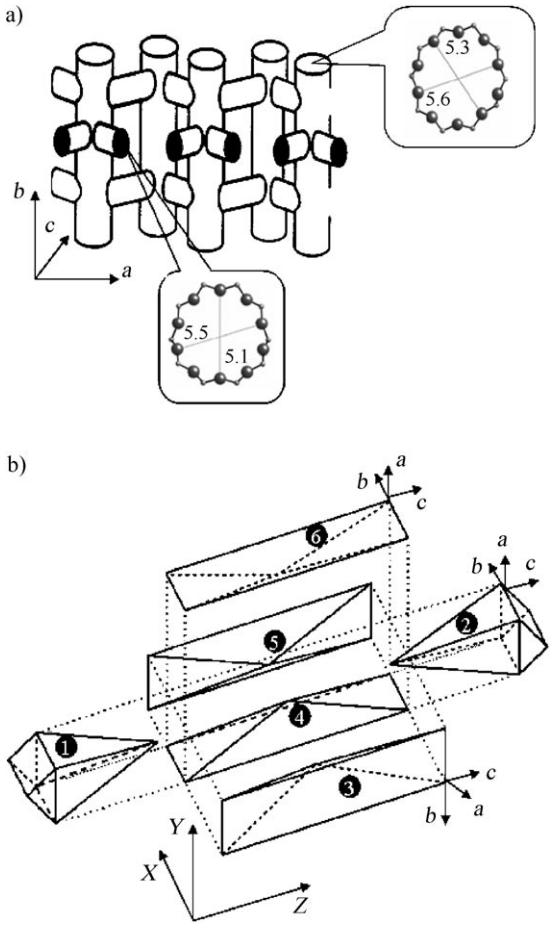


***Figure 1.*** Structure of the system under study. a) The three-dimensional pore system of silicalite-1, consisting of straight and zigzag channels. b) Schematic representation of the internal structure of silicalite-1 crystals; *x*, *y*, *z* indicate the crystal orientation, whereas *a*, *b*, *c* indicate the orientation of the pores in each segment.

[*] D. Tzoulaki, L. Heinke, Prof. Dr. J. Kärger
Department of Physics and Geoscience
University of Leipzig
Linnéstrasse 5, 04103 Leipzig (Germany)
Fax: (+49) 341-973-2549
E-mail: kaerger@physik.uni-leipzig.de
Homepage: http://ingo.exphysik.uni-leipzig.de/
Dr. W. Schmidt, U. Wilczok
Max-Planck-Institut für Kohlenforschung
Kaiser-Wilhelm-Platz 1, 45470 Mülheim an der Ruhr (Germany)

[**] This work has been financially supported by INDENS Marie Curie Program and by Deutsche Forschungsgemeinschaft. The authors would like to thank Christian Chmelik for stimulating discussions.

Supporting information for this article is available on the WWW under http://www.angewandte.org or from the author.

with those of segments 1 and 4, but not with those of 3 and 5. Within each individual crystal, the segments are arranged in such a way that only the zigzag channels reach the external surface, while the straight channels run parallel to the surface. In previous studies, the interfaces between the crystal segments could be identified as the source of intracrystalline transport resistance. Aluminum distributes inhomogeneously over large ZSM-5 crystallites. It is preferentially located close to the external surfaces of the crystallites. A similar enrichment of aluminum at the interfaces of the crystal segments could be postulated, this would result in enhanced catalytic activity and coke/polymer formation close to these interfaces, as observed in ref. [15,16]. This situation suggests that the diffusion barriers observed in these studies arise from pore blocking under reaction conditions.

Figure 2 provides an overview of the transient concentration profiles observed during uptake (Figure 2a and b) and release (Figure 2d) of isobutane initiated by a pressure step from 0 to 1 mbar (which corresponds to 2.8 molecules per unit cell)—and vice versa—in the surrounding atmosphere. Figure 2a shows the distribution of the concentration within the crystal. Figure 2b presents the profiles of the concentration integrals along the crystal $y$ direction at $z = 10$ μm. Figure 2d provides a comparison of the profiles during desorption, determined for different $z$ values. It is clear that the molecular uptake is essentially independent of $z$.

Most importantly, in both the adsorption and desorption runs, the boundary concentrations are found to assume the equilibrium values instantaneously. This result indicates that there is essentially no additional transport resistance ("surface barriers") on the outer crystal surface. In the case of silicalite-1 crystallites, surface barriers are probably amorphous silica layers on the exterior of the crystals. Prior to calcination, the silicalite-1 crystallites used were exposed to fresh, highly dilute sodium hydroxide solution for one day. During this alkaline treatment, thin amorphous silica layers easily dissolve, yielding surface-barrier-free crystallites. Complementary studies with crystals subject to a preceding leaching with fluoric acid[22] and with crystal fragments[17] (see Supplementary Information) confirm these findings.

Opposite to the case of one- and two-dimensional channel systems, for a three-dimensional case an analysis can no longer be based on the microscopic application of Fick's 2nd law[13] since the quantities now observed are nontrivial integrals of the concentration. Hence, the diffusion coefficients have to be determined by comparison of the observed concentration profiles with calculated profiles. These are generated by a numerical solution of Fick's 2nd law with suitably chosen concentration-dependent diffusion coefficient.[23] Diffusion in $x$- and $y$ direction is assumed to be essentially isotropic, while mass transport in the $z$ direction is assumed to be of negligible influence.[24,25] This assumption is confirmed experimentally by the absence of any concentration gradient along the $z$ direction.

The transport diffusion coefficient $D$ is the product of the thermodynamic factor $d(\ln p)/d(\ln c)$ determined from the equilibrium isotherm $c(p)$[26] and the corrected diffusion coefficient (also called the Maxwell–Stefan diffusion coefficient).[8] Best agreement with the observed concentration profiles of isobutane is obtained with a corrected diffusion coefficient of $1.05(1-0.52c) \times 10^{-12}\ m^2 s^{-1}$ with the transport diffusion coefficient increasing from $1.05 \times 10^{-12}\ m^2 s^{-1}$ to $1.7 \times 10^{-12}\ m^2 s^{-1}$. This finding nicely reproduces the values determined by molecular dynamics simulations[24] which, in the considered concentration range, gave the dif-

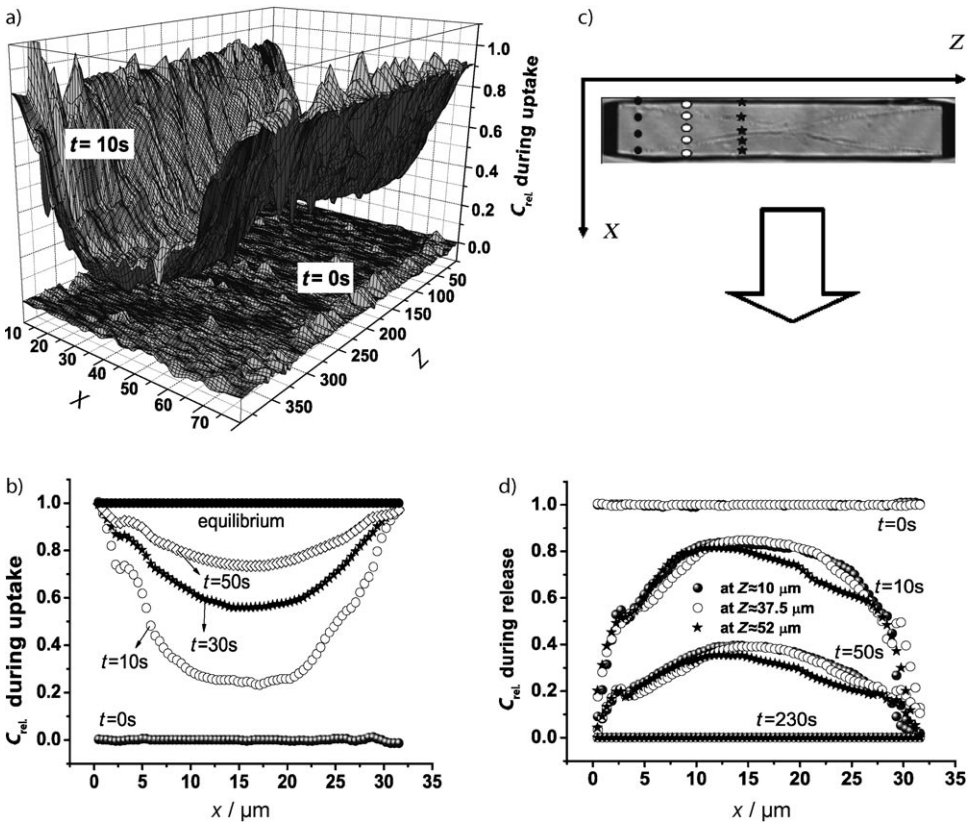


***Figure 2.*** Time-dependent concentration profiles of 2-methylpropane (isobutane) as a guest molecule in silicalite-1. a) two-dimensional concentration profile, 10 s after the onset of adsorption ($c_{rel}$: concentration normalized with saturation loading, namely with 2.8 molecules/u.c.). b) Evolution of the guest concentration profile along the $x$ axis at $z \approx 10$ μm during uptake. c) Host crystal with indication of the positions $z$ to which the concentration profiles in (d) refer. d) Evolution of the guest concentration profiles along the $x$ axis during release at different $z$ values.

  

fusion coefficient to be $4(1–0.5c)\times10^{-12}\,m^2s^{-1}$, and determined by the (macroscopic) ZLC (zero-length column) technique where at low loadings the diffusion coefficient is determined to $9.8\times10^{-13}\,m^2s^{-1}$.[27]

As an additional probe molecule we have chosen 2-methylbutane which, owing to its larger size, has a lower rate of uptake by, and release from, the pore system. Figure 3 shows both an overall two-dimensional concentration profile at a specific time during desorption (Figure 3a) and selected desorption profiles at different times at one $z$ value (Figure 3b). Figure 3c shows the profiles of the integrated concentration in the $x$ and $y$ directions. The agreement between these profiles confirms the regular crystal habit that is shown in Figure 1b and the validity of our assumption of diffusion isotropy in the $x$ and $y$ directions.

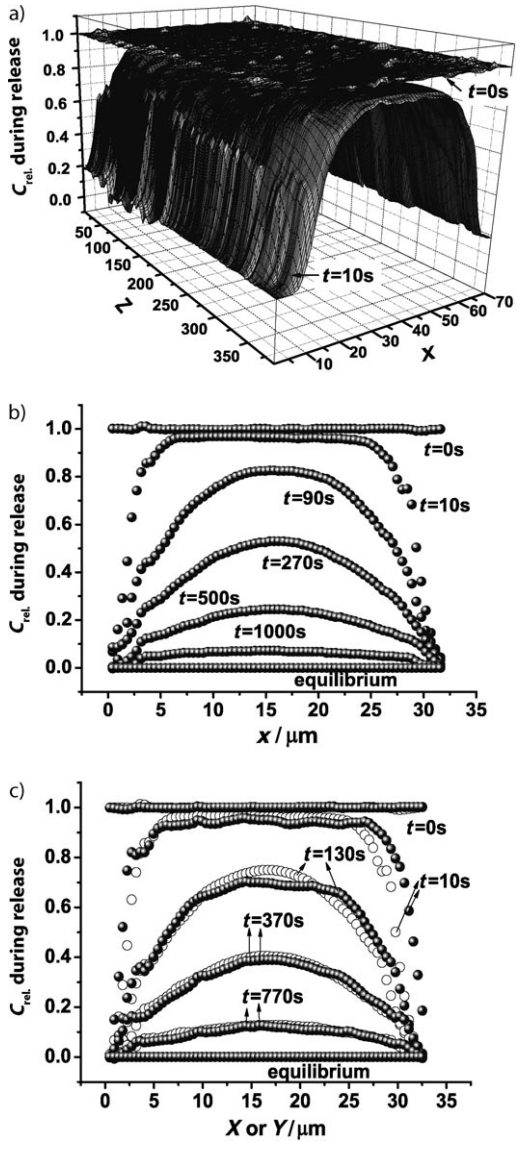


***Figure 3.*** Time-dependent concentration profiles of 2-methylbutane in silicalite-1; a) two-dimensional concentration profile, 10 s after the onset of adsorption. b) Evolution of the guest concentration profile along the $x$ axis at $z\approx10$ μm during release. c) Evolution of guest concentration profiles along $x$ axis (open symbols) and $y$ axis (filled symbols) at $z\approx10$ μm during release.

Using literature data for the adsorption isotherm,[28] the best agreement between the experimentally observed profiles of 2-methylbutane and the calculated ones is obtained for a corrected diffusion coefficient of $0.9(1–0.67c)\times10^{-13}\,m^2s^{-1}$ which corresponds to a transport diffusion coefficient increasing from $0.9\times10^{-13}\,m^2s^{-1}$ to $5\times10^{-13}\,m^2s^{-1}$.

Figure 4 illustrates that the calculated transient concentration profiles (full lines) satisfactorily reproduce the measured data. The best fit obtained with a concentration independent (that is, constant) diffusion coefficient, which allows an analytical interpretation (Figure 4, dotted lines), gives a somewhat larger deviation. The representations show that adsorption and desorption occur with comparable rates, which is in complete agreement with the observation that the profiles are not too different from those to be expected for constant diffusion coefficients.[8,24]

In summary, diffusion measurements by interference microscopy (using isobutane and 2-methylbutane as probe molecules) directly confirmed the regularity of the porous structure of MFI-type crystals. The results show that mass transport in a nanoporous host is not notably affected by internal transport resistances (i.e. at the interface between the intergrowth segments) or by a reduced permeability through the crystal surface (i.e. by surface barriers). In addition, our technique provides direct access to the magnitude of the transport parameters and their concentration dependence. Both types of information are essential for a complete material characterization and are often crucial for their technical applications.

## *Experimental Section*

The experimental set-up consists of a vacuum system, a microscope with camera and a computer. The interference microscope (Jenamap p dyn; Carl Zeiss GmbH) is equipped with an interferometer of the Mach-Zehnder type and a CCD camera, which digitizes the observed images.

The interferogram is generated from two light beams, one passing through the crystal and one through the surroundings (gas phase), respectively. These two beams are produced by the beam splitter of the interferometer and are superimposed so that an interference pattern is produced. This superposition reflects the difference of the optical path lengths through the crystal and the gas phase. The refractive index of a medium is a function of its composition. In this case, the "composition" of the crystal is represented by the concentration of guest molecules inside its pores. During uptake and/or release the concentration of guest molecules inside the crystal changes with time and, therefore, the refractive index $n_1$ changes as well. The difference optical densities $\Delta n$ (that is, between the $n_1$ and $n_2$ for the crystallite and its surroundings, respectively), gives rise to a phase difference in the respective beams [Eq. (1); where $x$, $y$, $z$ are three spatial coordinates, $t$ is the time, $\Delta s$ is the optical path length. The $x$ axis is the direction of observation and $L$ denotes the length of the crystal in this direction].

$$\Delta s(y,z,t) = \int_0^L \Delta n(x,y,z,t)\,dx \qquad (1)$$

Since the changes in the refractive index are very small, we may assume that the changes in the concentration and the refractive index of the crystal are proportional. Therefore, by using Equation (1), the experimental data (optical path length) yield a quantity which is

  

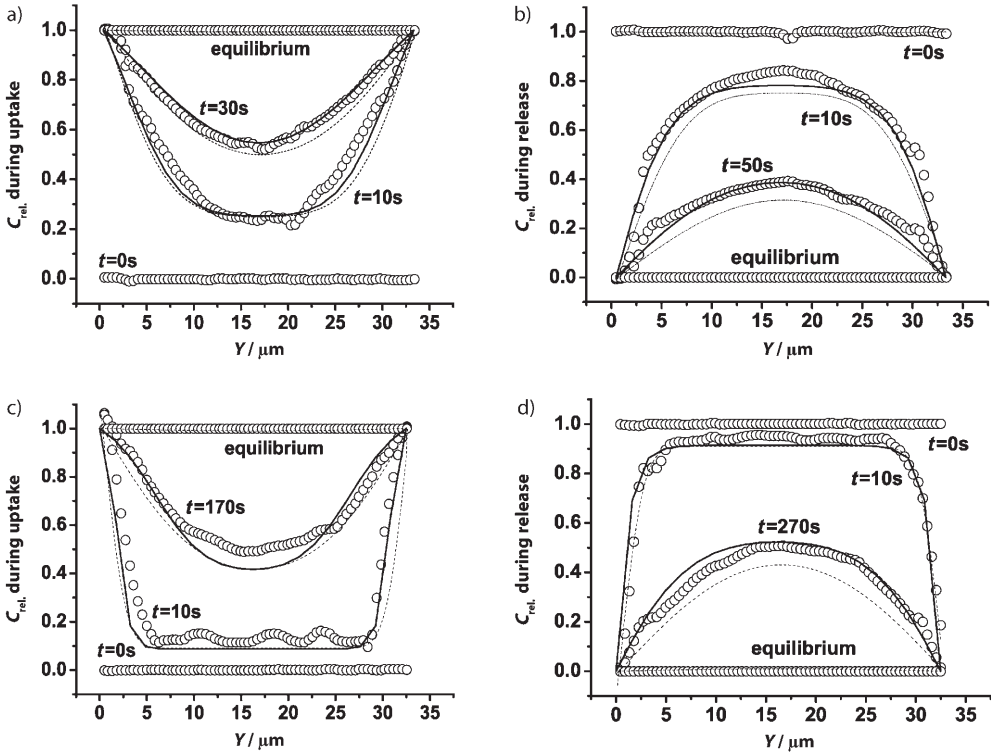


***Figure 4.*** Comparison of measured (symbols) and calculated (lines) time-dependent concentration profiles. The calculations have been performed with a concentration-dependent diffusion coefficient (solid lines) or with a constant diffusion coefficient (dashed lines; $D = 1.2 \times 10^{-12}\ m^2 s^{-1}$ for isobutane and $D = 1.7 \times 10^{-13}\ m^2 s^{-1}$ for 2-methylbutane). All profiles are along the *y* axis for $z \approx 10\ \mu m$. a) isobutane adsorption, b) isobutane desorption, c) 2-methylbutane adsorption, d) 2-methylbutane desorption.

proportional to the integral of the concentration in the direction of observation. The spatial resolution of this technique is $0.5 \times 0.5\ \mu m^2$ and the time resolution is 10 s. All experiments were performed at room temperature (295 K). Prior to each experiment, the whole system was evacuated and the sample activated according to the specific procedure appropriate for the given material (in our case for 12 h at 673 K).

Received: December 7, 2007
Published online: April 21, 2008

**Keywords:** diffusion · interference microscopy · silicalite-1 · surface resistance · zeolites

[1] R. M. Barrer, B. E. F. Fender, *J. Phys. Chem. Solids* **1961**, *21*, 12.
[2] R. M. Barrer, *Adv. Chem. Ser.* **1971**, *102*, 1.
[3] G. Arya, E. J. Maginn, H. C. Chang, *J. Phys. Chem. B* **2001**, *105*, 2725.
[4] M. Chandross, E. B. Webb G. S. Grest, M. G. Martin, A. P. Thompson, M. W. Roth, *J. Phys. Chem. B* **2001**, *105*, 5700.
[5] W. L. Duncan, K. P. Moller, *Adsorption* **2005**, *11*, 259.
[6] Y. Wang, M. D. Levan, *Adsorption* **2005**, *11*, 409.
[7] M. Bülow, *Z. Chem.* **1985**, *25*, 81.
[8] J. Kärger, D. M. Ruthven, *Zeolites* **1989**, *9*, 267.
[9] O. Geier, S. Vasenkov, E. Lehmann, J. Kärger, U. Schemmert, R. A. Rakoczy, J. Weitkamp, *J. Phys. Chem. B* **2001**, *105*, 10217.
[10] S. Vasenkov, W. Böhlmann, P. Galvosas, O. Geier, H. Lui, J. Kärger, *J. Phys. Chem. B* **2001**, *105*, 5922.
[11] P. Kortunov, S. Vasenkov, C. Chmelik, J. Kärger, D. M. Ruthven, J. Wloch, *Chem. Mater.* **2004**, *16*, 3552.
[12] E. Lehmann, S. Vasenkov, J. Kärger, G. Zadrozna, J. Kornatowski, Ö. Weiss, F. Schüth, *J. Phys. Chem. B* **2003**, *107*, 4685.
[13] J. Kärger, P. Kortunov, S. Vasenkov, L. Heinke, D. B. Shah, R. A. Rakoczy, Y. Traa, J. Weitkamp, *Angew. Chem.* **2006**, *118*, 8010; *Angew. Chem. Int. Ed.* **2006**, *45*, 7846.
[14] P. Kortunov, L. Heinke, M. Arnold, Y. Nedellec, D. J. Jones, J. Caro, J. Kärger, *J. Am. Chem. Soc.* **2007**, *129*, 8041.
[15] M. H. F. Kox, E. Stavitski, B. M. Weckhuysen, *Angew. Chem.* **2007**, *119*, 3726; *Angew. Chem. Int. Ed.* **2007**, *46*, 3652.
[16] M. B. J. Roeffaers, B. F. Sels, H. Uji-i, B. Blanpain, P. L'hoëst, P. A. Jacobs, F. C. De Schryver, J. Hofkens, D. E. De Vos, *Angew. Chem.* **2007**, *119*, 1736; *Angew. Chem. Int. Ed.* **2007**, *46*, 1706.
[17] W. Schmidt, U. Wilczok, C. Weidenthaler, O. Medenbach, R. Goddard, G. Buth, A. Cepak, *J. Phys. Chem. B* **2007**, *111*, 13538.
[18] J. Caro, M. Noak, J. Richter-Mendau, F. Marlow, D. Petersohn, M. Griepentrog, J. Kornatowski, *J. Phys. Chem.* **1993**, *97*, 13685.
[19] C. Weidenthaler, R. X. Fischer, R. D. Shannon, O. Medenbach, *J. Phys. Chem.* **1994**, *98*, 12687.
[20] M. Kocirik, J. Kornatowski, V. Masarik, P. Novak, A. Zikanova, J. Maixner, *Microporous Mesoporous Mater.* **1998**, *23*, 295.
[21] G. Müller, T. Narbeshuber, G. Mirth, J. A. Lercher, *J. Phys. Chem.* **1994**, *98*, 7436.
[22] M. Kocirik, P. Struve, K. Fiedler, M. Bülow, *J. Chem. Soc. Faraday Trans. 1* **1988**, *84*, 3001.
[23] J. Crank, *The Mathematics of Diffusion*, Oxford University Press, New York, 2nd ed., **1975**.
[24] A. Bouyermaouen, A. Bellemans, *J. Chem. Phys.* **1998**, *108*, 2170.
[25] J. Kärger, *J. Phys. Chem.* **1991**, *95*, 5558.
[26] D. Paschek, R. Krishna, *Chem. Phys. Lett.* **2001**, *342*, 148.
[27] W. Zhu, A. Malekian, M. Eic, F. Kapteijn, J. A. Moulijn, *Chem. Eng. Sci.* **2004**, *59*, 3827.
[28] R. Krishna, S. Calero, B. Smit, *Chem. Eng. J.* **2002**, *88*, 81.